



Cite this: *Environ. Sci.: Adv.*, 2023, **2**, 767

## Impact of iron oxide nanoparticles on a lead-polluted water–soil–plant system under alternating periods of water stress†

Léa Mounier,<sup>ab</sup> Mathieu Pédrot,<sup>b</sup> Martine Bouhnik-Le-Coz<sup>b</sup> and Francisco Cabello-Hurtado<sup>a\*</sup>

Iron oxide nanoparticles (IONPs) are promising materials for the remediation of trace elements, which are a significant source of soil pollution. Thus, in an attempt to improve the phytoremediation process, the addition of IONPs to soil was investigated in this study. A long-term experiment was performed in a pot to assess the potential of magnetite ( $Fe_3O_4$ ) nanoparticles (NPsMagn) to modify lead (Pb) availability in sunflower (*Helianthus annuus*) and its behavior in a water–soil–plant system under repeated water-deficiency stress. The plants were grown either in control soil, Pb polluted soil (final added lead  $375\text{ mg kg}^{-1}$ ), Pb-polluted soil containing 1% dry weight NPsMagn or Pb polluted soil containing 1% dry weight micro-sized magnetite for 90 days. The Pb-polluted soil and Pb-treated soil containing NPsMagn did not affect plant growth, whereas NPsMagn had a reduced oxidative impact given that a decrease in lipid peroxidation was observed in their presence. The magnetic susceptibility measurements and Fe content in sunflower plants and leachates suggest that NPsMagn penetrated the roots but were not dispersed in soil solution. In addition, the Pb content increased by 102% and 22% in the leaves and stems of the plants treated with NPsMagn, respectively. Based on the Pb content in soil solutions, NPsMagn decreased the Pb content in the leachate by 50%. During the water stress periods, NPsMagn significantly improved water retention in the soil and relative water content in the plants. Consequently, NPsMagn improved the Pb availability and accumulation in sunflower plants in TE-contaminated soils, which are unfavorable for plant growth. This study also highlights the favorable effects of NPsMagn on Pb stabilization in soil, reducing its loss in leachates and enhancing plant tolerance during water stress periods.

Received 18th November 2022  
Accepted 14th March 2023

DOI: 10.1039/d2va00283c  
[rsc.li/esadvances](http://rsc.li/esadvances)



### Environmental significance

Many sites are contaminated with lead, and consequently several types of remediation systems have been investigated. Among them, phytoremediation is environmentally friendly but slow, and thus we attempted to improve it with the addition of iron oxide nanoparticles. Indeed, magnetite nanoparticles, which are known for their high sorption capacity, can be used to influence Pb dynamics. This long-term study investigated the potential of magnetite nanoparticles for lead remediation in a complete cultivation system including water, soil and plant compartments. Influencing the mobility of Pb and impacting both soil, leached soil solution and plants, the findings show that magnetite nanoparticles are promising materials for trace element phytoremediation and plant stress tolerance, resulting in a decrease in the mobility of Pb in leachates, while increasing its bioavailability.

## 1. Introduction

Due to human activities, trace element (TE) pollution has become widespread and poses a threat to the environment and human health. Several million tons of TEs have been released in the environment during the last century<sup>1</sup> and have spread

worldwide even in remote ecosystems.<sup>2</sup> Among them, lead (Pb), mainly resulting from mining production, industries and transport, is one of the ubiquitously distributed most abundant toxic elements in soil and water without biological function.<sup>3</sup> In the last few decades, an estimated 783 000 tons of Pb have been dispersed in the environment worldwide.<sup>1</sup>

Through its bioaccumulation and nonbiodegradability, Pb soil contamination may cause significant hazards to human beings, animals and plants.<sup>4</sup> Lead has a strong effect on plants because it can impact all aspects of plant growth and health even at a very low concentration.<sup>5</sup> Plant germination has been shown to be inhibited<sup>6</sup> and biomass production of roots and aerial parts may also be affected.<sup>6–8</sup> Furthermore, Pb also

<sup>a</sup>Univ. Rennes 1, CNRS, ECOBIO, UMR 6553, Av. General Leclerc, F-35042 Rennes Cedex, France. E-mail: [francisco.cabello-hurtado@univ-rennes1.fr](mailto:francisco.cabello-hurtado@univ-rennes1.fr); Tel: +33 2 23235022

<sup>b</sup>Univ. Rennes 1, CNRS, Géosciences Rennes, UMR 6118, Av. General Leclerc, F-35042 Rennes Cedex, France

† Electronic supplementary information (ESI) available. See DOI: <https://doi.org/10.1039/d2va00283c>

impacts the metabolism of plants (e.g., decreasing photosynthetic activity, protein content, nutrient uptake, respiration rate and ATP content or increasing lipid peroxidation and oxidative stress).<sup>9</sup> ROS production caused by Pb toxicity may lead to oxidative stress, which is widely identified as an indicator of plant stress and may lead to cell death.<sup>10,11</sup> In some cases, Pb and TEs can be translocated from plants to the human dietary system, posing a major threat to human health.<sup>12</sup> Therefore, it has become necessary to take proactive measures to detoxify Pb-polluted soils.

Nanotechnology is an emerging field that covers a wide range of technologies currently being developed at the nano-scale. Among them, environmental nanotechnologies have enormous potential to provide innovative solutions to a wide range of environmental problems, including improved methods for pollution abatement, water treatment, environmental sensing and remediation, and making alternative energy sources more cost-effective.<sup>13</sup> The unique properties (e.g., small size and high surface area) of engineered nanomaterials enable these new technologies to address environmental challenges in a sustainable manner. The main objective of environmental nanotechnology also includes the safe design of nanomaterials with potential environmental benefits and the promotion of the sustainable development of these materials.<sup>14,15</sup> NPs such as iron oxide nanoparticles (IONPs) can interact with pollutants in soils and soil solutions, such as heavy metals, pesticides and other contaminants, and are promising materials for the stabilization of TEs.<sup>16</sup> For instance, IONPs have been applied for scavenging pollutants such as nitrate,<sup>17</sup> antibiotic medication,<sup>18</sup> and TEs such as Cr(vi),<sup>19</sup> Cd(II),<sup>20</sup> As(v),<sup>21</sup> Se(iv),<sup>22</sup> and Pb(II)<sup>23</sup> from aqueous media. Due to their high surface area, which promotes their sorption capacity, IONPs can influence the mobility, availability and toxicity of TEs, and in particular they limit the transport of Pb and the contamination of groundwater in case Pb is not absorbed by roots and soil particles.<sup>24</sup> Thus, IONPs effectively scavenge TEs and limit their transport through chemical mechanisms involving adsorption (both physical and chemical),<sup>25,26</sup> incorporation, and electron transfer (e.g., reduction of As(v) to As(III)),<sup>27,28</sup> For instance, Demangeat *et al.* observed that the increased Cu adsorption on IONPs was related to pH augmentation, which caused decreasing proton concentration at the magnetite surface, favoring cation attraction.<sup>29</sup> Under certain conditions, IONPs have been shown to decrease the toxicity of some TEs by decreasing their availability to plants.<sup>30</sup> The addition of IONPs significantly reduced the soluble Zn in the soil solution by 22%, demonstrating that IONPs acted by fixing Zn in the soil.<sup>30</sup>

In addition, the presence of IONPs can both influence the absorption and accumulation of TEs in plants, and also enhance plant growth through improved nutrition and fertilization.<sup>28,31</sup> Studies showed that NPs could enhance the plant capacity to absorb more nutrients and increase the efficiency of NPK use.<sup>32</sup> Also, organic matter (OM) can bind with IONPs (e.g., through hydrogen bonding, cation bridges and van der Waals interactions), and thus IONPs increase the amount of OM due to their high surface area.<sup>16</sup> The availability of iron for plant growth is also determined by the solubilization of Fe from iron-

rich minerals. This nutrient exchange is mediated by chemicals (pH and dissolution–precipitation) and biological (e.g., root exudate release) processes. Although it has been demonstrated that IONPs have limited penetration in plants, they aggregate on the surface of their roots.<sup>33</sup> Consequently, the accumulation of IONPs on roots can increase the bioaccumulation of the associated Pb. However, the processes underlying NP-mediated TE uptake and toxicity reduction vary with the NP type, mode of application, time of exposure and plant conditions (e.g., species, varieties, and development rate).<sup>14</sup> Current research is focused on the use of IONPs to reduce the phytotoxicity caused by toxic TEs<sup>34–36</sup> and improve plant growth.<sup>36,37</sup>

Thus, IONPs can be used in combination with plants for remediating soils contaminated by TEs; however, to take advantage of the potential of IONPs for remediation, issues concerning their availability, biocompatibility and behavior in soil and soil solution need to be further investigated. Sunflower (*Helianthus annuus*) was selected for the current study given that it has a high biomass production and promising phytoremediation potential due to its high ability to adsorb, stabilize and accumulate different concentrations of Pb<sup>38</sup> and tolerance to periods of water stress.<sup>39</sup> In this context, the objectives of this study were to (i) study the impact of both IONPs and Pb concerning their behavior in a water–soil–plant system, (ii) assess Pb phytoextraction potential by sunflower treated with IONPs, and (iii) evaluate the plant-protection capacities of IONPs under Pb pollution.

## 2. Materials and methods

### 2.1. Synthesis and characterization of iron oxide nanoparticles

Iron oxide nanoparticles, namely magnetite ( $Fe_3O_4$ ) nanoparticles (NPsMagn), were synthesized *via* the co-precipitation method<sup>40,41</sup> under aerobic conditions, and presented a size and surface area as that reported by Demangeat *et al.*<sup>29</sup> Briefly, a solution of  $FeCl_2$  and  $FeCl_3$  (1 : 2 molar ratio) was mixed with NaOH solution, leading to the precipitation of magnetite particles, and the solid phase was washed with ultrapure water. The final solution consisted of a non-stoichiometric magnetite  $Fe_{3-\delta}O_4$  with an  $Fe_{II}/Fe_{III}$  ratio in the range of 0.15 to 0.1, as determined by the spectrophotometric method described by Jungcharoen *et al.*<sup>42</sup> The size, shape, surface area and  $pH_{zpc}$  of NPsMagn were determined according to the methods described by Demangeat *et al.*<sup>29</sup> The synthesized NPsMagn possessed a round crystalline shape with a diameter of  $9 \pm 2$  nm (ESI Fig. S1†) and a specific surface area and  $pH_{zpc}$  of  $115 \text{ m}^2 \text{ g}^{-1}$  and 6.2, respectively. A micrometer-sized magnetite (particles  $< 5 \mu\text{m}$ ) ( $\mu$ Magn) solution was prepared by diluting magnetite (310 069 Sigma-Aldrich) in ultrapure water to the desired concentration.

### 2.2. Experimental design

A 90 day culture was performed with sunflower (*Helianthus annuus*) plants. The experimental set-up consisted of two nested pots (400 mL polypropylene beaker, Nalgene). The top pot



contained soil (335 g dry weight (DW) per pot) and a nylon cloth (31  $\mu\text{m}$  diameter) was added to its bottom to hold the soil particles in the higher part of the system. The top pot was pierced to allow the soil solution to run out and be collected in the second pot (ESI Fig. S2†). The soil used was collected on a grove-type site between the 10 to 20 cm-deep first horizon, homogenized and sieved to 5 mm diameter. Soil characterization was carried out (ESI, Table S1†) and the initial content in Pb determined (53.8 mg kg<sup>-1</sup> DW).

Four treatments of six replicates were performed for plant cultivation, as follows: unmodified soil (control), soil polluted with added Pb (Pb), soil polluted with added Pb and containing 1% NPsMagn (NPsMagn-Pb) and soil polluted with added Pb and containing 1% of micrometer-sized magnetite ( $\mu\text{Magn}$ -Pb). In addition, Pb and NPMagn-Pb treatments (three replicates each) were also studied without plants (soil Pb and soil NPsMagn-Pb, respectively). The soil was initially contaminated with added lead at a concentration of 150 mg kg<sup>-1</sup> of dry soil by adding 50 mL of 4.85 mM Pb(NO<sub>3</sub>)<sub>2</sub> per pot to the pristine soil and homogenized. This concentration is above toxicity threshold set in France<sup>43</sup> and corresponds to the toxicity limit in *H. annuus* found in the literature.<sup>7</sup> Three new additions of Pb(NO<sub>3</sub>)<sub>2</sub> corresponding to 75 mg Pb per kg soil each (at days 35, 42 and 49) brought the final added lead concentration to 375 mg kg<sup>-1</sup> soil. NPMagn solution (23 g L<sup>-1</sup>) was added to achieve 1% (m m<sup>-1</sup>) of dry soil to provide a consistent amount of material to achieve an optimal removal of TEs in soil according to Komárek *et al.*<sup>24</sup> Likewise, a micrometer-sized magnetite solution (25 g L<sup>-1</sup>) was added to the soil up to 1% (m m<sup>-1</sup>) of dry soil and homogenized.

Sunflower seeds were washed for 3 min in a 3% sodium hypochlorite bath, and then rinsed five times for 12 min in distilled water baths. Firstly, the seeds were sown in pristine soil and placed in a climatic chamber. After 18 days of growth, the young plants with the same state of growth were transplanted in the experimental set-up. The cyclic growth parameters of the climatic chamber included 16 h light at 21 °C and 8 h dark at 18 °C, a photosynthetic photon flux density of 160  $\mu\text{mol m}^{-2} \text{s}^{-1}$ , and relative humidity of 70%.

Each week, the soils were kept at field capacity with 0.5 mM NaCl solution for 4 days, followed by a period of 3 days of water deficit (absence of irrigation). Once a week, the soil solution was harvested by increasing the watering. For the pots cultivated with plants, the soil solutions collected from the six replicates were mixed two by two and homogenized at each sampling allowing to obtain a sufficient volume, and thus three samples per treatment were generated for geochemical analyses. In the case of the soil solutions from the non-cultivated pots, two samples were generated by dividing the soil solution of the second pot in two halves, and then each half was homogenized with the soil solution of pots 1 and 3, respectively.

After 90 days of culture, the plants were harvested for biological analysis. Pictures were taken, and the fresh weights of the roots, leaves and stem were measured for each one (if flower buds were present, they were counted with the leaves). The samples were frozen in liquid nitrogen and stored at -80 °C.

For NPMagn-Pb treatment, the roots and stem/leaves were vertically divided into three parts of equal length to assess the presence of NPsMagn in the plants *via* magnetic susceptibility measurement. The soil for each replicate was also collected and separated in three equal vertical parts for the magnetic susceptibility measurements. For the aerials parts, the 3 sections were named from bottom to top: "L1" (lower third), "L2" (mid third) and "L3" (upper third) for the leaves (T1, T2 and T3 for the stem). Similarly, the root (R1, R2 and R3) and soil (S1, S2, S3) parts were numbered from 1 to 3 with increasing depth.

### 2.3. Biological assays

To perform the biological analysis, the plant samples were first dried by lyophilization (Christ ALPHA 1-2LDplus), and then ground by milling (Mixer Mill MM400). The frozen samples were placed in the chamber for an initial long drying (0.09 Pa for 72 h), followed by a secondary short drying stage (0.001 Pa for 24 h). Dried vegetative samples were ground using zirconium bowls and beads.

**2.3.1. Pigment content.** To determine the chlorophyll and carotenoid contents, 5 mg DW of *H. annuus* leaves was added to 500  $\mu\text{L}$  of 80% acetone, mixed for 10 min at 4 °C and incubated in the dark for 12 h at 4 °C. After complete bleaching, the samples were centrifuged at 12 000g. The supernatant was recovered in new tubes, and 30  $\mu\text{L}$  was diluted in 270  $\mu\text{L}$  acetone (80%) in microplate wells. The pigment content was measured by spectrophotometrically reading the absorbance at 470, 645 and 663 nm (spectrometer SAFAS FLX-Xenius) and applying the equations of Lichtenthaler and Wellburn (1983).<sup>44</sup>

**2.3.2. Amino acid content.** To determine the amino acid content, the total amino acids were first extracted from 30 mg dried leaves with the addition of 1 mL ethanol (100%) and heated at 95 °C for 10 min with opened caps to allow the ethanol to evaporate, and then 1 mL ultra-pure water was added and centrifuged at 10 000g for 10 min at 4 °C. The supernatant was collected and stored at -20 °C.

The determination of total amino acids was performed following the method by Yemm *et al.*,<sup>45</sup> which was improved by Magné and Larher.<sup>46</sup> Briefly, 100  $\mu\text{L}$  of amino acid extract was added to 0.5 mL citrate buffer (177 mM, pH 4.6 containing 300 mM sodium hydroxide) and 1 mL of ninhydrin solution (47 mM ninhydrin, 50 mM ascorbic acid, ethanol (70% v/v)) and heated at 95 °C for 20 min. Then, 3 mL ethanol (70%) was added and absorbance at 570 nm was measured by spectrophotometry in a glass tank. Leucine was used to determine the amino acid content (calibration solution concentration in the range of 0 to 10 mM).

The proline content was determined following Troll and Lindsley's method.<sup>47</sup> Briefly, 100  $\mu\text{L}$  of amino acid extract was added to 1 mL of ninhydrin solution (6 mM ninhydrin, acetic acid (60% v/v)) and heated at 95 °C for 20 min. The samples were cooled in water for 15 min, 3 mL of toluene added and left for 1 h in the dark. After phase separation, the top solution was gently poured into a glass tank and its absorbance was measured at 520 nm.



**2.3.3. Determination of lipid peroxidation.** The quantification of lipid peroxidation products was achieved by measurement of thiobarbituric acid reactant species (TBARS) according to the corrected method proposed by Hodges *et al.*<sup>48</sup> Briefly, 1 mL ethanol (80%) was added to 15 mg dried leaves and left to react for 25 min in a rotation wheel at room temperature. After centrifugation for 10 min at 10 000g, the supernatant was collected in new tubes. Two aliquots of 200  $\mu$ L were prepared and 200  $\mu$ L of TBA+ solution (20% (w/v) trichloroacetic acid, 0.65% (w/v) TBA and 0.01% (w/v) butylhydroxytoluene) added. Two other aliquots were mixed with TBA-solution (20% (w/v) trichloroacetic acid and 0.01% (w/v) butylhydroxytoluene). The samples were heated at 95 °C for 25 min, and then centrifuged for 10 min at 10 000g after cooling at room temperature. The supernatant was recovered in new tubes, and 300  $\mu$ L was placed in microplate wells. The absorbance of the supernatant was measured at 440, 532 and 600 nm (spectrometer SAFAS FLX-Xenius) and results expressed in malondialdehyde equivalents (MDAeq) per gram of plant DW according to the equations by Hodges *et al.*<sup>48</sup>

**2.3.4. Soluble protein extraction and quantification.** For soluble protein extraction, 50 mg dry leaves were added to 1.5 mL sodium phosphate buffer (50 mM, pH 7.5) containing 1 mM Na-EDTA, 5% (w/v) polyvinylpyrrolidone, 0.5% (v/v) protease inhibitor cocktail (Sigma-P9599) and 0.1% (w/v) Triton X-100. The samples were shaken for 1 h at 4 °C, and then centrifuged twice at 12 000g for 12 min, and the supernatant was collected in new tubes. Soluble protein quantification was performed according to Bradford's method by spectrophotometric determination.<sup>49</sup> Bovine serum albumin (BSA) was used to determine the protein contents (calibration solution range was 0.1 to 1.4 mg L<sup>-1</sup>). The protein extracts were kept at -80 °C for further use in the POD and SOD enzymatic antioxidant activity assays.

**2.3.5. Determination of POD activity.** Guaiacol peroxidase (POD) activity was determined based on modified literature procedures.<sup>50</sup> The reaction was performed in a microplate containing the reaction mixture of 190  $\mu$ L deionized ultrapure water, 30  $\mu$ L potassium phosphate buffer (1 M, pH 6.5), 30  $\mu$ L guaiacol (150 mM) and 50  $\mu$ L soluble protein extract. The reaction was triggered by the addition of 30  $\mu$ L of H<sub>2</sub>O<sub>2</sub> (160 mM) and monitored by reading the absorbance at 470 nm ( $\epsilon_{\text{tetraguaiacol}} = 26.6 \text{ mM}^{-1} \text{ cm}^{-1}$ ) for 6 min. The observed increase in absorbance provided the maximum rate of tetra-guaiacol formation and was used to determine the enzymatic activity. The amount of enzyme that reduced 1 mmol of H<sub>2</sub>O<sub>2</sub> per min corresponds to 1 unit (U) of POD under the assayed conditions.

**2.3.6. Determination of SOD activity.** The capacity of superoxide dismutase (SOD) to inhibit the photochemical reduction of nitro blue tetrazolium (NBT) was measured following the modified method of Giannopolitis and Ries.<sup>51</sup> Each microplate well was filled with 175  $\mu$ L deionized ultrapure water, 30  $\mu$ L potassium phosphate buffer (500 mM, pH 7.8), 30  $\mu$ L of methionine (130 mM), 30  $\mu$ L of NBT (750  $\mu$ M) and 5  $\mu$ L of soluble protein extract. Two microplates were prepared, one

exposed to light and one kept in the dark (for light-independent reactions corrections) for spectrometric analysis. A pre-reading of each plate was realized at 560 nm before initiating the reaction. Then, 30  $\mu$ L of riboflavin (20  $\mu$ M) was added in each well to start the reaction and the samples were exposed either to light (30 min) or kept in the dark. The absorbance was measured at 560 nm, and pre-read values were subtracted from the final absorbance measurement. The SOD activity is expressed in U mg per protein, with "U" corresponding to the amount of enzyme causing 50% inhibition of the NBT reduction to blue formazan observed in the absence of the enzyme.

#### 2.4. Leaf angle measurement

The photos used for the measurement of leaf angle were taken twice a week at the beginning and the end of the water stress periods. The leaf inclination angle was measured using the ImageJ software and corresponds to the angle between the abaxial face of the leaf and the petiole (measurements were made on four leaves per plant).

#### 2.5. Relative water content

To determine the relative water content (RWC), 10 leaf discs (1 cm diameter) were collected and their fresh weights (FW) measured. The leaf discs were immersed for 24 h in distilled water, and then their turgescence weights (TW) were assessed. The leaf discs were heated at 70 °C for 48 h and their DW determined. The RWC was evaluated according to the following equation: RWC = ((FW-DW)/(TW-DW)) × 100.

#### 2.6. Geochemical analyses

The pH was measured using a combined Mettler InLab electrode after calibration was performed with 3 standard buffers (pH 4, 7, and 10). The redox potential was measured with a Pt electrode combined with an Ag/AgCl reference electrode (Fisher Scientific Bioblock). The  $E_h$  values are presented in millivolts relative to the standard hydrogen electrode, including a correction measurement using a commercial redox buffer (220 mV vs. Ag/AgCl). The soil solutions were filtered at 0.2  $\mu$ m with syringe filters to remove particles. 10 mL of the filtered soil solutions was directly acidified by sub-boiled nitric acid (HNO<sub>3</sub>; 14.6 N) at 2% v/v for ICP-MS analysis, and the remainder stored at 4 °C.

**2.6.1. Trace element measurements.** The lead and iron concentrations were determined by ICP-MS (Agilent 7700×) using rhenium and rhodium as internal standards. The international geostandard SLRS-6 was used to check the validity and reproducibility of the results. The typical uncertainties including all error sources were below  $\pm 5\%$  for Fe and Pb. The samples were prepared in a clean room and the tubes were pre-washed (24 h in 1.5 M HNO<sub>3</sub> at 45 °C, 24 h in deionized ultrapure water at 45 °C).

For the biological samples, 5 mL 14.6 N sub-boiled HNO<sub>3</sub>, 1 mL 37% H<sub>2</sub>O<sub>2</sub> and 1 mL ultrapure water were added to 100 mg plant DW in specific digestion tubes (Anton Paar Teflon 18 mL vials). The samples were digested using a multi-wave (Multiwave 7000 Anton Paar) and a specific program. In the first step, the temperature was increased to 250 °C for 20 min at 140 bars, and



then kept at 250 °C for 30 min at 140 bars. Next, the digested solutions were transferred to digestion vessels (Savillex Teflon vials) and heated until the solvent evaporated. The samples were dissolved in 0.37 M sub-boiled HNO<sub>3</sub> with appropriate dilution(s) considering the ICP-MS quantification limits.

**2.6.2. Determination of dissolved organic carbon.** The amount of dissolved organic carbon (DOC) was determined using a Total Organic Carbon Analyzer (TOC-L SHIMADZU). The accuracy of the DOC measurement was estimated at  $\pm 3\%$  (using a standard solution of potassium hydrogen phthalate).

**2.6.3. Determination of soil water potential.** The soil water potential was determined using a WP4C dew point meter (METER Group, Inc). The measurements were performed on soil taken after plant harvest in each treatment. The same amount of soil was filled in the WP4C sample cup and placed in the block chamber of WP4C for measurement.

## 2.7. Magnetic susceptibility measurements

To confirm the presence of magnetite in the environment, magnetic susceptibility was previously used.<sup>52</sup> Here, magnetic susceptibility measurements were conducted to track and quantify NPsMagn in different parts of the sunflower plants and in the soil. The analyses were performed using a magnetic susceptibility meter (Kappabridge AGICO KLY3).

To perform the measurements, the samples were dried by lyophilization and stored in clean plastic containers. To account for the container signal, blanks (containers without samples) were used at the beginning and end of the acquisitions and after every 10 measurements. To ensure the validity and reproducibility of the results, the magnetic susceptibility measurements were repeated 12 times for each sample. Then, the mass susceptibilities ( $\text{m}^3 \text{ kg}^{-1}$ ) were calculated considering the sample weight. Based on these values, the concentration of NPsMagn in the samples was determined based on the blank-corrected magnetic susceptibility of a sample of NPsMagn of known weight.

## 2.8. Statistical analysis

Each value is presented as the mean  $\pm$  standard error of the mean (SEM), with at least 3 replicates. Normality was confirmed with the Shapiro test and homoscedasticity with the Bartlett test for each assay. Statistical analyses were conducted using the Tukey test (ANOVA) or Kruskal-Wallis test to assess the significance of the means with  $p < 0.05$  considered significant. The significantly different data are indicated with different letters.

# 3. Results and discussion

## 3.1. Physiological and biochemical responses of *Helianthus annuus* plants exposed to NPsMagn in a Pb pollution context

**3.1.1. Growth parameters.** After 90 days of plant growth, no significant difference was observed for either the dry weight of leaves or stems (Fig. 1) and plant height (average 55 cm, data not shown) between the control plants and plants submitted to any of the treatments.

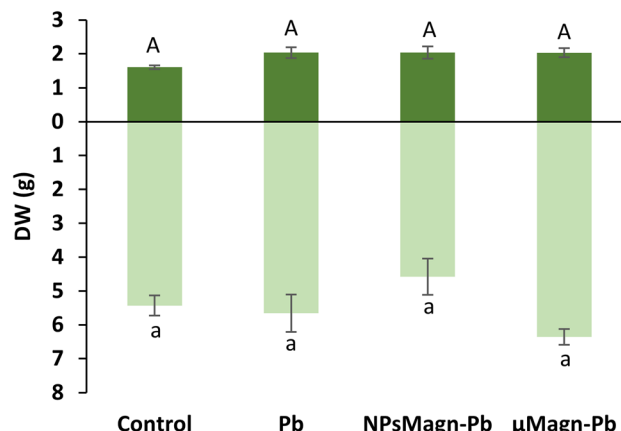


Fig. 1 Dry weight (g) of leaves (dark green) and stems (light green) of sunflower plants measured after 90 days of growth on control soil or containing Pb, NPsMagn-Pb or  $\mu$ Magn-Pb. Data represent the mean  $\pm$  SEM ( $n = 6$ ). Different letters indicate significant differences between treatments for each plant organ ( $p < 0.05$ ).

Even if NPMagn-Pb treatment did not promote a significant increase in aerial biomass, our results show the harmlessness of the NPMagn treatment at remediation concentrations (1%)<sup>24</sup> in Pb-polluted soils, which is in agreement with recent research in our laboratory concerning the impact of NPsMagn on sunflower plants under Cu pollution.<sup>52</sup> However, it is possible that the action of NPsMagn is affected by different factors such as the application concentration, plant species, duration of the experiment, culture medium, and plant development stage.<sup>53</sup> Also, it can be considered that the size of the experimental set-up used may have been a limiting factor in the plant development, given that sunflowers can reach much greater heights and biomass in the environment. In the present study, even if 1% NPsMagn did not impact the growth, the initiation of the flower buds was affected because the buds were present in all the plants exposed to NPsMagn-Pb and they were more developed than in the other treatment groups after 90 days of growth. Indeed, no flower buds were observed for the control treatment, and only one and two flower buds out of six plants in  $\mu$ Magn-Pb and Pb, respectively. In contrast, previous work<sup>52</sup> showed a delay in the flowering of sunflowers treated with NPsMagn and no flowering at all for sunflowers germinated and grown with NPsMagn under Cu pollution. However, in this study,<sup>52</sup> the seeds were put to germinate directly in contact with the various treatments, which could have caused a global growth delay in the case of NPMagn treatments.

Furthermore, here, the presence of Pb in the soil at a final added concentration of 375 mg kg<sup>-1</sup> soil did not impact the leaf or stem biomass production, which is in contrast to that found in the literature.<sup>7,54</sup> However, Madejón *et al.* showed a different impact of TEs, including Pb, on the growth of sunflower according to the stage of development of the plant.<sup>55</sup> Soil pollution significantly retarded the early growth of the youngest plant (1 month after sowing), especially root growth. In our experimental set-up, even if only an estimate of root biomass was made because the whole roots could not be precisely and



equally recovered from the soil (ESI Fig. S3†), visual observation provided a sufficient basis to note that root growth was impacted by Pb pollution. In contrast, Madejón *et al.* found no differences in sunflower biomass production after 130 days of growth in Pb-contaminated soil ( $113 \text{ mg kg}^{-1}$ ) compared to the control.<sup>55</sup> Given that we introduced 18 day-old seedlings into the experimental set-up, it is likely that the aerial parts were not impacted by Pb because they had already passed this critical growth period.

**3.1.2. Pigment contents.** For each condition, the contents of chlorophylls (Ca and Cb) and carotenoids (K) followed the same pattern (Fig. 2). In the case of the plant growth parameters, the leaves of the plants exposed to Pb contained similar pigment levels to the control. The highest content was found after  $\mu\text{Magn-Pb}$  treatment, under which the pigment contents were roughly one third higher than that in the control. In contrast, the pigment contents were significantly lower in NPsMagn-Pb than in the Pb and  $\mu\text{Magn-Pb}$  treatments (Fig. 2), and the Ca/Cb ratio decreased by 11% in NPsMagn-Pb compared to the control leaves (Fig. 2). However, despite these differences in pigment contents, none of the treatments affected the maximum quantum yield of photosynthesis (ESI Table S2†).

Several studies reported that IONPs can affect the pigment concentrations of exposed plants.<sup>56</sup> Among them, for sunflower, a previous work found that NPsMagn diminished the chlorophyll and carotenoid contents up to 50% in sunflower seedlings and the combination with Pb contributed to increase this impact.<sup>57</sup> Besides, IONPs can induce no effect<sup>58</sup> or increase<sup>59</sup> the pigment contents.

It has also been documented that photosynthesis inhibition is a result of Pb toxicity due to the varying effects of Pb according to plant species, including inhibition of chlorophyll and carotenoid synthesis, distorted chloroplast ultrastructure, obstruction of the electron transport system, inhibition of Calvin cycle enzymatic catalysis, impaired uptake of essential elements such as Mn and Fe and substitution of divalent

cations by Pb, or increased chlorophyllase activity.<sup>9</sup> Nevertheless, this impact is affected by the Pb dose in combination with soil properties, as will be discussed later (Section 3.2.2).

**3.1.3. Concentrations of total free amino acids.** The amount of total free amino acids is equivalent among treatments ( $6 \mu\text{g g}^{-1}$  DW), except for NPsMagn-Pb, in which the total free amino acids was higher by 50% (Fig. 4). Given that Pb alone seems to have no impact on the sunflower amino acid content (Fig. 4), it is likely that NPsMagn have an effect on primary metabolite production. Zahra *et al.*<sup>60</sup> reported that the external addition of NPs can change the level of most amino acids in plants. They observed that the use of  $\text{TiO}_2$  NPs in wheat induced an increase in amino acid production. The cessation of sugar biosynthesis, due to the disruption of photosynthesis, shifted the cellular metabolism to the use of amino acids as an alternative energy source.<sup>61</sup> Also,  $\text{Fe}_2\text{O}_3$  NPs induced an increase in cysteine and tyrosine content in wheat.<sup>62</sup>

**3.1.4. Oxidative stress response.** TBARS (such as malondialdehyde, MDA) result from the decomposition of unstable and reactive lipid peroxides produced by lipid peroxidation, which occurs in cells after oxidative stress.<sup>48</sup> Given that the TBARS content reflects the degree of oxidative injury to a plant cell, a decreased TBARS content is inferred to result from the absence of oxidative injury from the treatment applied. The TBARS content in NPsMagn-Pb was similar to that in the control, while this amount was significantly higher by 21% in the Pb and  $\mu\text{Magn-Pb}$  treatment (Fig. 3A). Thus, NPsMagn likely provided or induced protection against lipid peroxidation caused by lead treatment, which was not observed for  $\mu\text{Magn}$ . Demangeat *et al.*<sup>52</sup> showed a similar pattern of lipid peroxidation reduction in sunflower plants when exposed to NPsMagn or NPsMagn-Cu compared to Cu treatment. This protective effect of IONPs against lipid peroxidation has also been demonstrated for other plant species.<sup>37,63</sup>

POD and SOD are some of the enzymes that participate in protection mechanisms against oxidative damage. We did not observe significant differences in POD or SOD activities between treatments, except for POD activity in the Pb-treated plants, which is twice that in the control group (Fig. 3B and C). Increasing the activities of SOD and POD has been shown to provide better mechanisms for protecting plants from oxidative damage.<sup>64</sup> In particular, POD, by catalyzing the reaction between  $\text{H}_2\text{O}_2$  and ROOH to  $\text{H}_2\text{O}$  and R-OH, directly protects against cellular damage.<sup>65</sup> In their study, Demangeat *et al.*<sup>52</sup> showed a correlation between a decrease in TBARS content and increase in antioxidant POD activity in NPMagn-Cu-treated plants, suggesting that the POD antioxidant response acts effectively against ROS under Cu exposure. In our study, the lower POD and TBARS contents seem to indicate less oxidative stress in the plants under NPMagn-Pb treatment, highlighting the protective effect of NPsMagn. Interestingly, as already mentioned, the amino acid content was higher in the NPMagn-Pb-treated plants (Fig. 4). It has been shown that under stress conditions, abundant amino acids are synthesized to help plants to cope with stress-provoked imbalances.<sup>66</sup> Alternatively, the two-fold increase in POD and TBARS content with Pb treatment suggests that the plant cells probably accumulated

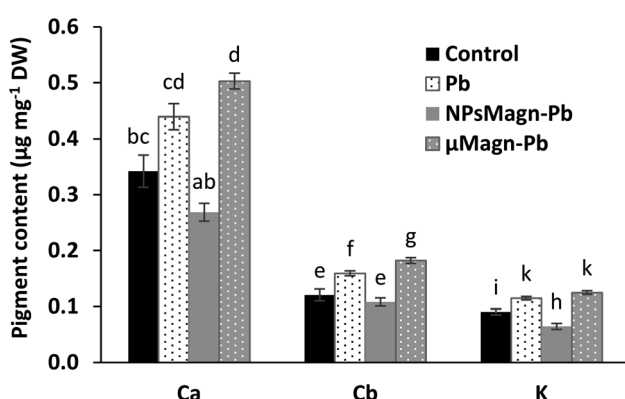


Fig. 2 Pigment content ( $\mu\text{g mg}^{-1}$  DW) measured in the leaves of sunflower plants after 90 days of growth on control soil or containing Pb, NPsMagn-Pb or  $\mu\text{Magn-Pb}$ . Data represent the mean  $\pm$  SEM ( $n = 6$ ) of the pigment content measured in the leaves of sunflowers grown for 90 days in the different studied soils. Different letters above the bars indicate significant differences ( $p < 0.05$ ).



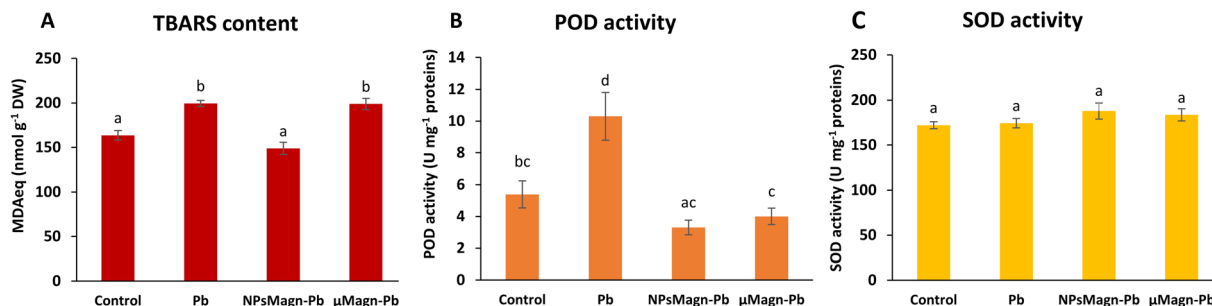


Fig. 3 Lipid peroxidation and antioxidant activities measured in the leaves of sunflower plants after 90 days of growth on control soil or containing Pb, NPsMagn-Pb or μMagn-Pb. (A) TBARS content (nmol MDAeq per g DW); (B) POD activity (U mg per protein); and (C) SOD activity (U mg per protein). Data represent the mean  $\pm$  SEM ( $n = 6$ ). Different letters above the bars indicate significant differences ( $p < 0.05$ ).

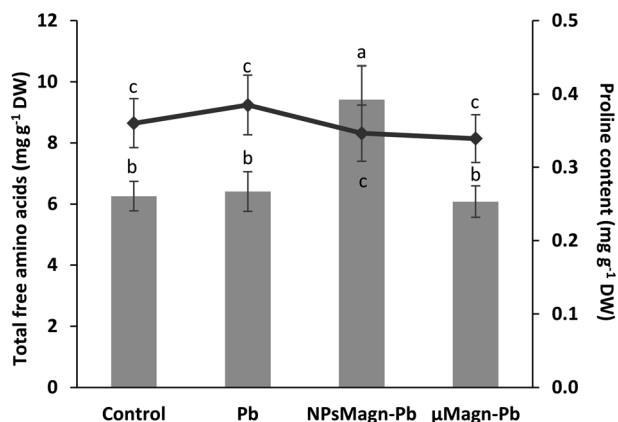


Fig. 4 Total free amino acids (mg<sub>eq</sub> leucine g<sup>-1</sup> DW) (histogram) and proline content (mg g<sup>-1</sup> DW) (curve) measured in the leaves of sunflower plants after 90 days of growth on control soil or containing Pb, NPsMagn-Pb or μMagn-Pb. Data represent the mean  $\pm$  SEM ( $n = 6$ ). Different letters above the bars indicate significant differences ( $p < 0.05$ ).

more ROS in response to Pb pollution, which caused lipid peroxidation of the membranes and induced antioxidant mechanisms to cope.

### 3.2. Fate of NPsMagn and Pb in a water-soil-plant system

**3.2.1. Uptake and translocation of NPsMagn from soil to plant.** Iron was mainly found in the leaves, where its levels varied from 34 mg kg<sup>-1</sup> DW (control) to 38 mg kg<sup>-1</sup> DW (NPsMagn-Pb) but no significant differences in Fe content in the sunflower leaves were observed between treatments (Fig. 5A). Even if the Fe content in the stems was lower than that in the leaves, regardless of the treatment, it was significantly higher by 23% in the stems of plants treated with NPsMagn-Pb compared to the control (Fig. 5A). In contrast, the Fe content in the stems significantly decreased by 18% in μMagn-Pb condition compared to the control.

Concerning the fate of NPsMagn in the soil, no significant differences between treatments were found in the magnetic susceptibility measurements in soil, suggesting that NPsMagn did not migrate over time with the leachates (Table 1). NPsMagn

tended to aggregate to mm-sized particles and this tendency may have resulted in their decreased mobility in the soil,<sup>67</sup> in addition to their bonding to clays and organic matter (OM) in the soil because of their high affinity for each other.<sup>67</sup>

Previous studies in the literature reported that NPs accumulated primarily at the root level, before entering the upper parts of the plant.<sup>33</sup> Here, based on the magnetic susceptibility measurements, NPsMagn were detected in the roots but not the aerial parts of the sunflower plants grown in the NPMagn-Pb-contaminated soil. The NPMagn content in the roots significantly decreased from the top to bottom (Table 1). Given that the concentration of NPsMagn in the soil did not change with depth, the possibility of their absorption inside the roots and displacement with water flow, and not just adsorption on the sunflower roots as observed by Demangeat *et al.*<sup>52</sup> must be considered to explain the root distribution of NPsMagn (Table 1). The adsorption of NPsMagn on the roots is due to their positive surface charges, which are more likely to adsorb and accumulate on the negatively charged root surfaces.<sup>68</sup> Alternatively, depending on their size, NPs can penetrate the roots through the pores of the cell wall, and then follow the apoplastic pathway to reach the vascular tissue. From the central cylinder (including the xylem and phloem), NPs can reach the aerial parts of plants by following the transpiration flow.<sup>69</sup> Based on the data in Fig. 5 and Table 1, we cannot confirm the presence of NPsMagn in the aerial tissues of the sunflowers. However, the significant increase in Fe in the whole aerial part and stems of the plants grown in NPMagn-Pb media evidenced the possible occurrence of a small amount of NPsMagn in the sunflower stems. The translocation of NPsMagn in plants varies among studies. They were either be found in barley aerial parts and roots without cellular penetration<sup>70</sup> or detected in pumpkin leaves and roots, in stems close to the roots and on the root surface.<sup>71</sup> In contrast, they were not translocated in ryegrass.<sup>72</sup>

As observed in Fig. 5B, the cumulative amount of Fe released in the NPMagn-Pb soil solution was eight-times higher than that in the soil solutions of the control soil. However, it is worth mentioning that the amount of Fe leached after 75 days only represented 0.04% of the Fe present in the soil. These results corroborate that observed by Demangeat *et al.*,<sup>52</sup> emphasizing that leaching had little effect on the mobility of NPsMagn in the soil. An important increase in the iron release in leachates took



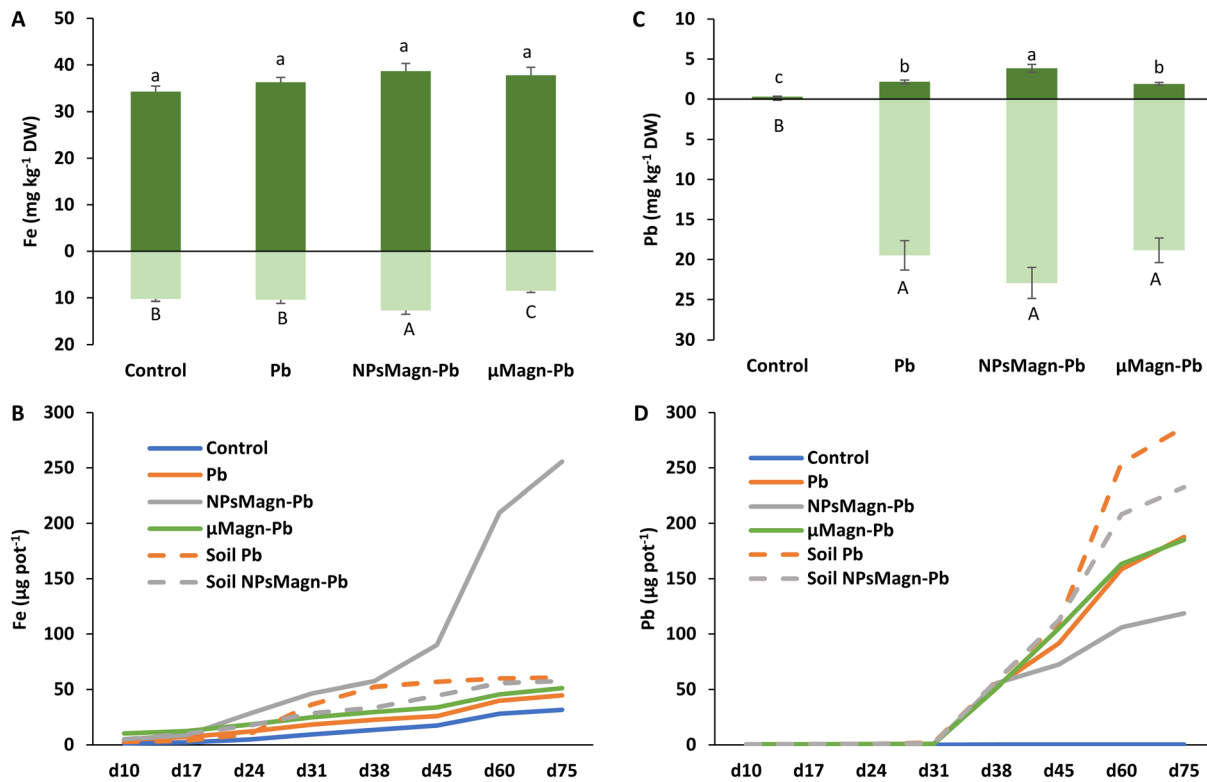


Fig. 5 Iron (A) and lead (C) concentrations ( $\text{mg kg}^{-1}$  DW) in leaves (dark green) and stems (light green) measured by ICP-MS after 90 days of growth in the different studied soils. Data represent the mean  $\pm$  SEM ( $n = 6$ ). Different letters above or below the bars indicate significant differences between treatments for each plant organ ( $p < 0.05$ ). Cumulative amounts of iron (B) and lead (D) leached ( $\mu\text{g}$  per pot) over the experimental period (day 10 to day 75) measured by ICP-MS. Dotted lines represent treatments without plant. Data represent the mean ( $n = 2$ ).

Table 1 Magnetite nanoparticle concentration ( $\text{mg kg}^{-1}$ ) in sunflower roots and aerial parts, and in the soil samples, calculated from magnetic susceptibility measurements. Soil samples and sunflower plants were harvested after 90 days of exposure to NPsMagn-Pb. The quantification limit (QL) was determined at  $40 \text{ mg kg}^{-1}$ . Data represent the mean  $\pm$  SEM ( $n = 6$ ). Different letters above indicate significant differences among plant or soil parts ( $p < 0.05$ )

NPsMagn-Pb		
Leaves	L1	<QL
	L2	<QL
	L3	<QL
Stem	T1	<QL
	T2	<QL
	T3	<QL
Roots	R1	$3319 \pm 493^a$
	R2	$1895 \pm 435^b$
	R3	$1074 \pm 164^b$
Soil	S1	$8171 \pm 267^a$
	S2	$8587 \pm 296^a$
	S3	$8202 \pm 383^a$

place from day 45 of the experiment in the NPMagn-Pb treatment group. No pH or redox potential changes explaining this behavior before and after their release were observed and the redox potential values were similar to other treatments. These patterns were not observed in the leachates from the treatments without plants, suggesting that plants play a role in iron release

in the media. In fact, root exudates (e.g., organic acids, sugars, amino acids, and proteins) or microbial activity (e.g., iron-reducing bacteria) may foster the dissolution of NPsMagn and Fe release into more bioavailable forms (such as that induced by the action of (phyto)siderophores).<sup>73</sup> In the context of the environmental fate and ecotoxicity of IONPs, our results highlight the low dispersion of NPsMagn in the soil and the importance of the presence of a vegetation cover.

**3.2.2. Chemical exchange among plants, soil and soil solution.** With the input of Pb in the soils, the amount of Pb increased in the plant stems and leaves (Fig. 5C) and in the leaching solutions (Fig. 5D). In all the aerial parts of the sunflowers, the Pb content tended to be higher when the plants were grown in soil treated with NPsMagn-Pb than in that treated with Pb or μMagn-Pb (Fig. 5C). The Pb content in the leaves increased significantly by 78% and 102% in the sunflowers treated with NPsMagn compared to the plants in the Pb and μMagn-Pb treatment groups, respectively. Furthermore, the Pb content in the stems was 6- to 9-times higher than that in the leaves, with a maximum for the treatment with NPsMagn ( $22.93 \text{ mg kg}^{-1}$ ). Similar results were observed in rice, where Pb accumulated three-times more in the stems.<sup>74</sup> The results indicated that the addition of NPsMagn in an appropriate amount to achieve an optimal removal of TEs could effectively increase the accumulation capacity of Pb in the studied plant. Previous findings indicated an increase in Pb accumulation



capacity by *Kochia scoparia* in nano zero valent iron-amended soil up to a specific concentration of nanomaterials, beyond which, the Fe nanoparticle effect on Pb accumulation decreased.<sup>75</sup> They observed adverse effects of high concentrations of nano zero valent iron in soil on total Pb accumulation capacity of *K. scoparia*. In contrast, in another study, the reduced accumulation of Pb in plant-soil system treated with compost added with maghemite nanoparticles.<sup>30</sup>

Remarkably, the leaching of Pb decreased by 37% and 20% in the Pb-contaminated soil enriched with NPsMagn relative to the soil without NPsMagn, respectively, both with and without sunflower plants (Fig. 5D). Within the same treatment, the presence of plants considerably affected the amount of Pb leached in the soil solution. Thus, the lead content also decreased by 35% and 50% in the presence of plants in the Pb and NPMagn-Pb treatments compared to a similar set-up without plants, respectively. The crop cover prevented the dispersion of TEs by water and wind erosion, and reduced their mobility and bioavailability.<sup>76</sup> Phytostabilisation can occur depending on diverse processes (e.g., sorption, precipitation, complexation and valence reduction)<sup>77</sup> and is controlled by various components (such as, pH and redox potential, OM content, soil texture, soil structure and microorganisms).<sup>78</sup> TEs mainly accumulate at the rhizospheric level and in the roots tissues depending of several factors such as root exudates, presence of microorganisms in the rhizosphere, binding of TEs on the cell wall or with metal binding molecules or their accrual in the vacuoles.<sup>79</sup>

In addition, IONPs have high affinity for Pb depending on the environmental conditions.<sup>80</sup> Thus, IONPs retained Pb in the soil and limited its dispersion in the soil solution as expected. In the treatments without plants, the soil pH was higher (pH 5.74 for cultivated soil and pH 6.45 for non-cultivated soil), leading to a higher release of colloids to which Pb is bound.<sup>81</sup> Indeed, the impact of plants on the leachate components can also be seen in Fig. 6, where the amount of dissolved organic carbon (DOC) is significantly higher by 92% (soil Pb) and 106%

(soil NPsMagn-Pb) in the leachates from the set-up without plants compared to their counterparts with plants. Interestingly, even if the Pb proportion in the leachates represents less than 0.2% of the total amount in soil, the Pb concentration in the leachates (e.g., 503 and 342  $\mu\text{g L}^{-1}$  in cumulated leachates from Pb and NPsMagn-Pb treatments, respectively, data not shown) and Pb retention by NPsMagn are relevant considering lead exposure through water sources.<sup>82</sup>

Moreover, it is worth noting that the Pb adsorption by NPsMagn did not limit the Pb uptake by the plant (Fig. 5C). At the rhizospheric level, Pb penetrates the roots *via* the apoplastic pathway or through  $\text{Ca}^{2+}$  permeable channels.<sup>9</sup> We also hypothesized that the binding of NPsMagn to the roots of the sunflowers enhanced the Pb uptake by the plants by making rhizospheric Pb more bioavailable. Concerning the root exudates, Luo *et al.* showed that amino acids such as alanine and proline could influence Pb uptake by *Sedum alfredii*.<sup>83</sup> Finally, even if no growth improvement was observed, the plants treated with NPsMagn-Pb were thriving as well as the control or Pb-treated plants but with higher amounts of Pb in their aerial parts.

Furthermore, as discussed above, the amount of DOC was significantly higher in the leachates from the set-up without plants compared to that with plants. Although in the presence of plants, the NPMagn-Pb treatment did not impact the DOC amount in the leachates, the DOC in the leachates increased by 115% and 167% for Pb and  $\mu\text{Magn-Pb}$  compared to the control, respectively. To date, few studies have been conducted on the influence of OM on the surface reactions of IONPs. OM and IONPs interact mainly through the adsorption of OM on their particle surface, and this adsorption has a significant impact on the adsorption of other ions and molecules.<sup>84</sup> Our results highlight that Pb seems to increased the OM leaching, and conversely the addition of NPsMagn decreased the OM loss in the leachates. In addition, as discussed above for Pb leaching, the presence of plants in the experimental set-up seemed to prevent OM leaching. Poirier *et al.* reviewed the link between the root characteristics and soil OM stabilization processes.<sup>85</sup> They identified several roots traits that participate in retaining OM in soil, as follows: (i) accumulation in the rhizosphere of root molecules recalcitrant against decomposition (e.g., root suberin<sup>86</sup>), (ii) occlusion in soil aggregates, which limits access to microorganisms and enzymes, and (iii) interaction with soils minerals and metals (formation of stable organo-mineral associations).<sup>87</sup> Also, high root lengths and density<sup>88</sup> are key factors in the stabilization of OM given that they can entangle and aggregate soil particles<sup>89</sup> and stimulate microbial activity by producing exudates, which act as a binding agent.<sup>90</sup>

### 3.3. Water stress response during interaction with NPsMagn-Pb

Research on NPs is growing, but few studies have investigated the relationship between NPs and rhizospheres as well as plant-water relations. However, the response of plants to water stress is a crucial element in their interactions with TEs. Recent studies on the application of NPs under water stress in plants

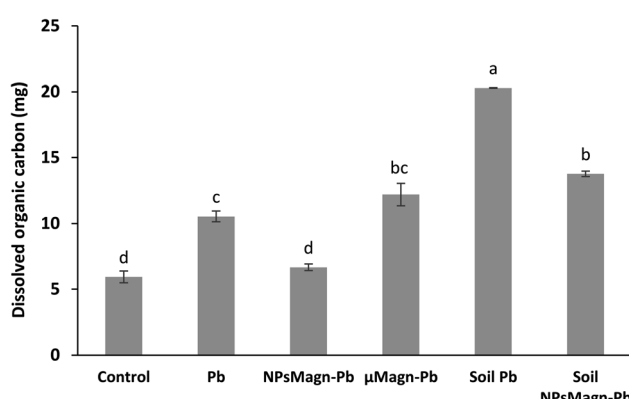


Fig. 6 Total amount of dissolved organic carbon leached over the experiment (mg). Leachates were filtered at 0.2  $\mu\text{m}$  with syringe filters to dissociate the particulate from the dissolved phase. Data represent the mean  $\pm$  SEM ( $n = 6$ ). Different letters above the bars indicate significant differences ( $p < 0.05$ ).



show promising results.<sup>91</sup> Thus, we sought to evaluate the impact of NPsMagn on the water relations in our cropping system in response to water stress through different measurements. In each water stress period, all plants showed visual symptoms of water deficit but it was significantly less pronounced in the sunflowers treated with NPsMagn. Different measurements were performed to further investigate this observation. Firstly, we determined the soil water potential, which corresponds to a pressure measurement quantifying the energy level of the water molecules in a solution. The water potential of the NPMagn-treated soil was four-times higher after 3 days water stress than that of the control soil (Fig. 7A). It is likely that the addition of a nanoparticulate fraction (1%) modified the soil structure, given that clay minerals increase the water reserve of the soil due to their high surface area. Ajayi and Horn tested the addition of 2%, 5% and 10% of clay (bentonite) in fine sand, which led to an increase in water holding capacity.<sup>92</sup> This can be explained by the increasing internal surface area of the amended soil,<sup>93</sup> availability of binding sites, and mineralogy of the clay material.<sup>92,94</sup> Thus, water can be

stored in the soil macropores, attracted to the outer surfaces of clay minerals, or retained as intercalated water in spaces between clay layers.

In addition, we can expect that IONPs, which can bind to OM, can potentially promote soil water retention to a certain threshold over long period. The results in Fig. 6 (Section 3.2.2) confirm that DOC is more retained in the soil in the presence of NPsMagn. These results support the hypothesis that NPsMagn can improve the water retention in soil.<sup>95</sup>

In the search for easily measurable indicators of water stress, we analyzed the effects of water stress periods on the leaf angle. The evolution of the leaf angle according to the field capacity (FC) or water deficiency (WD) periods showed that the plants in each treatment group followed the same pattern except for that exposed to NPsMagn (Fig. 7B). Thus, the leaf angle of the control plants varied with an increase in plant age in the range of  $106^\circ \pm 2^\circ$  to  $90^\circ \pm 4^\circ$  during the FC periods and from  $28^\circ \pm 2^\circ$  to  $74^\circ \pm 5^\circ$  during the WD periods. Specifically, the angle decreased from 73% to 25% for the water stress periods starting at the 56<sup>th</sup> and 84<sup>th</sup> days of plant culture, respectively. In contrast, the leaf angles of the plants exposed to NPsMagn varied from  $111^\circ \pm 5^\circ$  to  $105^\circ \pm 2^\circ$  in FC and in the range of  $56^\circ \pm 3^\circ$  to  $107^\circ \pm 2^\circ$  in WD, and thus a significant reduction in leaf angles from 49% to 2% for water stress periods starting at the 56<sup>th</sup> and 84<sup>th</sup> days of plant culture, respectively. In addition, we also evaluated the leaf relative water content (RWC) under water stress periods. Given that the RWC reflects the balance between the water supply to the leaf and transpiration rate, this is an important indicator of water status in plants.<sup>96</sup> Interestingly, we determined that only in the presence of NPsMagn the leaf RWC was significantly higher compared to the control (Fig. 7A).

Finally, in the case of water stress, the determination of proline content was used as an indicator of stress in the plants.<sup>97</sup> Here, no difference in proline content was noted (Fig. 4). In their study on nano-maghemit, Martínez-Fernández *et al.* did not find any difference among treatment in RWC, leaf surface area and proline content in sunflowers under water stress.<sup>30</sup> As in their study, we did not observe the production of proline as a stress response marker, but rather with the leaf angle and RWC and measurements on soil water potential. Even if some NPs have been shown to have a deleterious impact at the root level by mechanically disrupting the cell membrane and wall, thus affecting water absorption by the roots,<sup>98</sup> in other cases, NPs improved the tolerance to water stress by affecting different physiological and biochemical mechanisms such as improvement in photosynthetic parameters, regulation of stomatal conductance, antioxidant activity, nutrient and water use efficiency or osmolyte content.<sup>91</sup> For instance, the application of different metal oxide NPs in soybean improved the biomass reduction rate, RWC and drought tolerance index,<sup>99</sup> and IONP treatment enhanced the biomass, photosynthesis efficiency, nutrient uptake and antioxidant enzyme content in *Oryza sativa*.<sup>100</sup>

Overall, our results show that NPsMagn seemed to have a considerable impact on the soil structure and water retention, which indirectly influenced the plant physiology. However, further studies are needed to describe these structural changes

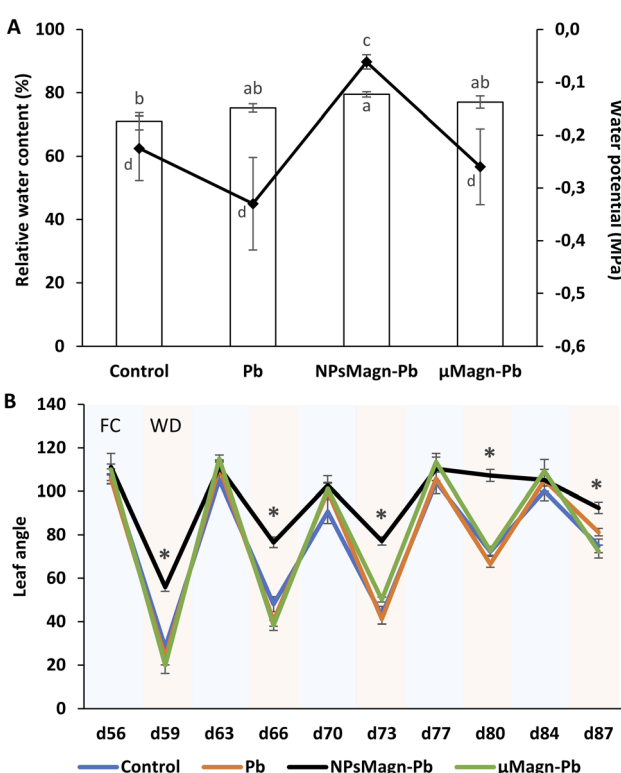


Fig. 7 Stress water response measured during and after 90 days of growth on control soil or containing Pb, NPsMagn-Pb or  $\mu$ Magn-Pb. (A) Water potential (histogram) of the different studied soils measured by WP4C dew meter point after plants harvest and relative water content (%) (curve) measured in the leaves of sunflower plants after 90 days of growth. (B) Leaf angle measured at different times of culture (FC = field capacity, pale blue; WD = water deficiency, pale pink). Measurements correspond to the angle between the abaxial face of the leaf and the petiole. Data represent the mean  $\pm$  SEM ( $n = 6$  or 12 for leaves angle). Different letters above the bars indicate significant differences ( $p < 0.05$ ). An asterisk indicates significant difference with control ( $p < 0.05$ ).



more precisely. In addition, gene expression analysis in plants treated with NPs under water stress conditions is a new avenue to explore because different studies show that the application of NPs under water stress induces an increase in the expression of drought-responsive genes.<sup>99,101</sup> Thus, the improvement in drought tolerance can be mediated by triggering the expression of drought-related genes *via* NPs.

## 4. Conclusions

In conclusion, even at high concentrations as that recommended for remediation, NPsMagn had little impact on the growth and on some physiological and biochemical responses of sunflower, and instead showed a protective effect against oxidative impact. Moreover, NPsMagn seemed to enhance (i) the Pb availability and accumulation in plants, given that a higher amount of Pb was measured in the sunflower aerial parts and (ii) Pb stabilization in the soil, given that a smaller amount of Pb was determined in the soil leachates. Likewise, the Fe content was superior in the plants treated with NPsMagn, and NPsMagn decreased the loss of soil dissolved organic matter and Pb transfer in the leachates. Finally, here, we showed that the plants treated with NPsMagn presented an improved water stress response and leaf water status, which could be partially explained by the enhanced retention of water in the soils containing NPsMagn. All these results indicate that NPsMagn are promising materials for TE remediation purposes, and thus promising avenues of research, particularly for the agricultural sector, where water stress is one of the main causes of loss. However, further research is needed to understand the underlying mechanisms, especially at the molecular level. These data provide new answers where the knowledge about the environmental fate and toxicity of nanoparticles is still inadequate.

## Author contributions

LM: conceptualization, methodology, validation, resources, formal analysis, investigation, data curation, writing – original draft, visualization. MBLC: methodology, validation, investigation. MP: conceptualization, methodology, validation, writing – review & editing, supervision, funding acquisition. FCH: conceptualization, methodology, validation, writing – review & editing, supervision, funding acquisition, project administration.

## Conflicts of interest

Authors declare no conflicts of interest.

## Acknowledgements

This work was supported by the SURFNANO project funded by the CNRS-INSU EC2CO program and the SynFeSol project funded by the Brittany Region (AAP TRANSFERT 2019). Through the support of the GeOHeLiS analytical platform of Rennes University, this publication is also supported by the European

Union through the European Regional Development Fund (FEDER), the French Region of Brittany and Rennes Metropole. We also thank THEMIS plateform and Laura Fablet for their contribution to the TEM images acquisition as well as Pierrick Roperch for magnetic susceptibility analyses. Léa Mounier was supported by a doctoral research grant from the University of Rennes 1 – French Ministry of Higher Education and Research.

## References

- 1 O. V. Singh, S. Labana, G. Pandey, R. Budhiraja and R. K. Jain, *Appl. Microbiol. Biotechnol.*, 2003, **61**, 405–412.
- 2 G. S. Senesil, G. Baldassarre, N. Senesi and B. Radina, *Chemosphere*, 1999, **39**, 343–377.
- 3 A. Kushwaha, N. Hans, S. Kumar and R. Rani, *Ecotoxicol. Environ. Saf.*, 2018, **147**, 1035–1045.
- 4 A. Kumar, A. Kumar, M. Cabral-Pinto, A. K. Chaturvedi, A. A. Shabnam, G. Subrahmanyam, R. Mondal, D. K. Gupta, S. K. Malyan, S. S. Kumar, S. A. Khan and K. K. Yadav, *Int. J. Environ. Res. Public Health*, 2020, **17**, 2179.
- 5 E. S. Perl, *Int. J. Phytorem.*, 2020, **22**, 916–930.
- 6 E. Islam, X. Yang, T. Li, D. Liu, X. Jin and F. Meng, *J. Hazard. Mater.*, 2007, **147**, 806–816.
- 7 P. Chauhan, A. B. Rajguru, M. Y. Dudhe and J. Mathur, *Environ. Technol. Innovation*, 2020, **18**, 100718.
- 8 F. Hadi, A. Bano and M. P. Fuller, *Chemosphere*, 2010, **80**, 457–462.
- 9 B. Pourrut, M. Shahid, C. Dumat, P. Winterton and E. Pinelli, in *Reviews of Environmental Contamination and Toxicology*, ed. D. M. Whitacre, Springer New York, New-York, 2011, vol. 213, pp. 113–136.
- 10 E. Keunen, T. Remans, S. Bohler, J. Vangronsveld and A. Cuypers, *Int. J. Mol. Sci.*, 2011, **12**, 6894–6918.
- 11 A. Kumar and M. N. V. Prasad, *Ecotoxicol. Environ. Saf.*, 2018, **166**, 401–418.
- 12 N. Natasha, M. Shahid, S. Khalid, I. Bibi, M. A. Naeem, N. Niazi, F. Tack, J. Ippolito and J. Rinklebe, *Crit. Rev. Environ. Sci. Technol.*, 2021, **16**, 1–41.
- 13 G. Ali Mansoori, T. R. Bastami, A. Ahmadpour and Z. Eshaghi, *Annu. Rev. Nano Res.*, 2008, **2**, 439–493.
- 14 M. Rizwan, S. Ali, M. Z. ur Rehman, M. Riaz, M. Adrees, A. Hussain, Z. A. Zahir and J. Rinklebe, *Ecotoxicol. Environ. Saf.*, 2021, **221**, 112437.
- 15 A. Latif, D. Sheng, K. Sun, Y. Si, M. Azeem, A. Abbas and M. Bilal, *Environ. Pollut.*, 2020, **264**, 114728.
- 16 C. Claudio, E. di Iorio, Q. Liu, Z. Jiang and V. Barrón, *J. Nanosci. Nanotechnol.*, 2017, **17**, 4449–4460.
- 17 Z. Jiang, L. Lv, W. Zhang, Q. Du, B. Pan, L. Yang and Q. Zhang, *Water Res.*, 2011, **45**, 2191–2198.
- 18 J. Chen, X. Qiu, Z. Fang, M. Yang, T. Pokeung, F. Gu, W. Cheng and B. Lan, *Chem. Eng. J.*, 2012, **181–182**, 113–119.
- 19 L. Alidokht, A. R. Khataee, A. Reyhanitabar and S. Oustan, *Desalination*, 2011, **270**, 105–110.
- 20 H. K. Boparai, M. Joseph and D. M. O'Carroll, *J. Hazard. Mater.*, 2011, **186**, 458–465.



21 H. Zhu, Y. Jia, X. Wu and H. Wang, *J. Hazard. Mater.*, 2009, **172**, 1591–1596.

22 L. Liang, W. Yang, X. Guan, J. Li, Z. Xu, J. Wu, Y. Huang and X. Zhang, *Water Res.*, 2013, **47**, 5846–5855.

23 X. Zhang, S. Lin, Z. Chen, M. Megharaj and R. Naidu, *Water Res.*, 2011, **45**, 3481–3488.

24 M. Komárek, A. Vaněk and V. Ettler, *Environ. Pollut.*, 2013, **172**, 9–22.

25 M. Auffan, J. Rose, O. Proux, D. Borschneck, A. Masion, P. Chaurand, J.-L. Hazemann, C. Chaneac, J.-P. Jolivet, M. R. Wiesner, A. Van Geen and J.-Y. Bottero, *Langmuir*, 2008, **24**, 3215–3222.

26 J. Tang, M. Myers, K. A. Bosnick and L. E. Brus, *J. Phys. Chem. B*, 2003, **107**, 7501–7506.

27 T. Borch, R. Kretzschmar, A. Kappler, P. V. Cappellen, M. Ginder-Vogel, A. Voegelin and K. Campbell, *Environ. Sci. Technol.*, 2010, **44**, 15–23.

28 S. U. Rahman, X. Wang, M. Shahzad, O. Bashir, Y. Li and H. Cheng, *Environ. Pollut.*, 2022, **310**, 119916.

29 E. Demangeat, M. Pédro, A. Dia, M. Bouhnik-Le-Coz, M. Davranche and F. Cabello-Hurtado, *Environ. Pollut.*, 2020, **257**, 113626.

30 D. Martínez-Fernández, M. Vítková, M. P. Bernal and M. Komárek, *Water, Air, Soil Pollut.*, 2015, **226**, 101.

31 M. Kah, N. Tufenkji and J. C. White, *Nat. Nanotechnol.*, 2019, **14**, 532–540.

32 C. O. Dimkpa, J. C. White, W. H. Elmer and J. Gardea-Torresdey, *J. Agric. Food Chem.*, 2017, **65**, 8552–8559.

33 X. Ma, J. Geiser-Lee, Y. Deng and A. Kolmakov, *Sci. Total Environ.*, 2010, **408**, 3053–3061.

34 Fahad, A. Balouch, M. H. Agheem, S. A. Memon, A. R. Baloch, A. Tunio, Abdullah, A. H. Pato, M. S. Jagirani, P. Panah, A. A. Gabole and S. Qasim, *Int. J. Environ. Anal. Chem.*, 2020, 1–12.

35 A. Konate, X. He, Z. Zhang, Y. Ma, P. Zhang, G. M. Alugongo and Y. Rui, *Sustainability*, 2017, **9**, 790.

36 M. Rui, C. Ma, Y. Hao, J. Guo, Y. Rui, X. Tang, Q. Zhao, X. Fan, Z. Zhang, T. Hou and S. Zhu, *Front. Plant Sci.*, 2016, **7**, 815.

37 N. G. M. Palmqvist, G. A. Seisenbaeva, P. Svedlindh and V. G. Kessler, *Nanoscale Res. Lett.*, 2017, **12**, 631.

38 P. Chauhan and J. Mathur, *Journal of Biological Sciences and Medicine*, 2018, **4**, 5–16.

39 F. Karam, R. Lahoud, R. Masaad, R. Kabalan, J. Breidi, C. Chalita and Y. Roushail, *Agric. Water Manag.*, 2007, **90**, 213–223.

40 E. Demangeat, M. Pédro, A. Dia, M. Bouhnik-le-Coz, F. Grasset, K. Hanna, M. Kamagata and F. Cabello-Hurtado, *Environ. Sci.: Nano*, 2018, **5**, 992–1001.

41 R. Massart, *IEEE Trans. Magn.*, 1981, **17**, 1247–1248.

42 P. Jungcharoen, M. Pédro, F. Choueikani, M. Pasturel, K. Hanna, F. Heberling, M. Tesfa and R. Marsac, *Environ. Sci.: Nano*, 2021, **8**, 2098–2107.

43 *Journal Officiel République Française*, 1998, <https://www.legifrance.gouv.fr/jorf/id/JORFTEXT000000206637/>, accessed September 2020.

44 H. K. Lichtenhaler and A. R. Wellburn, *Biochem. Soc. Trans.*, 1983, **11**, 591–592.

45 E. W. Yemm, E. C. Cocking and R. E. Ricketts, *Analyst*, 1955, **80**, 209.

46 C. Magné and F. Larher, *Anal. Biochem.*, 1992, **200**, 115–118.

47 W. Troll and J. Lindsley, *J. Biol. Chem.*, 1955, 215–655.

48 D. M. Hodges, J. M. DeLong, C. F. Forney and R. K. Prange, *Planta*, 1999, **207**, 604–611.

49 M. M. Bradford, *Anal. Biochem.*, 1976, **72**, 248–254.

50 I. Cakmak and H. Marschner, *Plant Physiol.*, 1992, **98**, 1222–1227.

51 C. N. Giannopolitis and S. K. Ries, *Plant Physiol.*, 1977, **59**, 309–314.

52 E. Demangeat, M. Pédro, A. Dia, M. Bouhnik-Le-Coz, P. Roperch, G. Compaoré and F. Cabello-Hurtado, *Nanoscale Adv.*, 2021, **3**, 2017–2029.

53 M. Amde, J. Liu, Z.-Q. Tan and D. Bekana, *Environ. Pollut.*, 2017, **230**, 250–267.

54 Z. Rengel, *Mechanisms of Environmental Stress Resistance in Plants*, CRC Press, 1997.

55 P. Madejón, J. Murillo, T. Maranon, F. Cabrera and M. Soriano, *Sci. Total Environ.*, 2003, **307**, 239–257.

56 D. K. Tripathi, Shweta, S. Singh, S. Singh, R. Pandey, V. P. Singh, N. C. Sharma, S. M. Prasad, N. K. Dubey and D. K. Chauhan, *Plant Physiol. Biochem.*, 2017, **110**, 2–12.

57 M. Ursache-Oprisan, E. Focanici, D. Creanga and O. Caltun, *Afr. J. Biotechnol.*, 2011, **36**, 7092–7098.

58 Y. Wang, S. Wang, M. Xu, L. Xiao, Z. Dai and J. Li, *Environ. Pollut.*, 2019, **249**, 1011–1018.

59 M. H. Ghafariyan, M. J. Malakouti, M. R. Dadpour, P. Stroeve and M. Mahmoudi, *Environ. Sci. Technol.*, 2013, 10645–10652.

60 Z. Zahra, N. Waseem, R. Zahra, H. Lee, M. A. Badshah, A. Mehmood, H.-K. Choi and M. Arshad, *J. Agric. Food Chem.*, 2017, **65**, 5598–5606.

61 S. Silva, T. P. Ribeiro, C. Santos, D. C. G. A. Pinto and A. M. S. Silva, *J. Hazard. Mater.*, 2020, **399**, 122982.

62 Y. Wang, F. Jiang, C. Ma, Y. Rui, D. C. W. Tsang and B. Xing, *J. Environ. Manage.*, 2019, **241**, 319–327.

63 M. F. Iannone, M. D. Groppa, M. E. de Sousa, M. B. Fernández van Raap and M. P. Benavides, *Environ. Exp. Bot.*, 2016, **131**, 77–88.

64 T. Abedi and H. Pakniyat, *Czech J. Genet. Plant Breed.*, 2010, **46**, 27–34.

65 J. Patykowski and J. Kołodziejek, *Pol. J. Environ. Stud.*, 2016, **25**, 725–732.

66 T. M. Hildebrandt, *Plant Mol. Biol.*, 2018, **98**, 121–135.

67 M. Al-Sid-Cheikh, M. Pédro, A. Dia, M. Davranche, L. Jeanneau, P. Petitjean, M. Bouhnik-Le Coz, M.-A. Cormier and F. Grasset, *Environ. Sci.: Nano*, 2019, **6**, 3049–3059.

68 J. Lv, P. Christie and S. Zhang, *Environ. Sci.: Nano*, 2019, **6**, 41–59.

69 A. Pérez-de-Luque, *Front. Environ. Sci.*, 2017, **5**, 5–12.

70 H. Tombuloglu, Y. Slimani, G. Tombuloglu, M. Almessiere and A. Baykal, *Chemosphere*, 2019, **226**, 110–122.



71 H. Zhu, J. Han, J. Q. Xiao and Y. Jin, *J. Environ. Monit.*, 2008, **10**, 685–784.

72 H. Wang, X. Kou, Z. Pei, J. Q. Xiao, X. Shan and B. Xing, *Nanotoxicology*, 2011, **5**, 30–42.

73 S. Bastani, R. Hajiboland, M. Khatamian and M. Saket-Oskoui, *J. Soil Sci. Plant Nutr.*, 2018, **18**, 524–541.

74 U. Ashraf, M. H.-R. Mahmood, S. Hussain, F. Abbas, S. A. Anjum and X. Tang, *Chemosphere*, 2020, **248**, 126003.

75 A. Daryabeigi Zand and A. Mikaeili Tabrizi, *Environ. Eng. Res.*, 2020, **26**, 200227.

76 N. S. Bolan, J. H. Park, B. Robinson, R. Naidu and K. Y. Huh, in *Advances in Agronomy*, Elsevier, 2011, vol. 112, pp. 145–204.

77 M. Ghosh, *Appl. Ecol. Env. Res.*, 2005, **3**, 1–18.

78 V. Chaignon, D. Di Malta and P. Hinsinger, *New Phytol.*, 2002, **154**, 121–130.

79 A. M. Shackira and J. T. Puthur, in *Plant-Metal Interactions*, ed. S. Srivastava, A. K. Srivastava and P. Suprasanna, Springer International Publishing, Cham, 2019, pp. 263–282.

80 J.-F. Liu, Z.-S. Zhao and G.-B. Jiang, *Environ. Sci. Technol.*, 2008, **42**, 6949–6954.

81 M. Pédrot, A. Dia and M. Davranche, *J. Colloid Interface Sci.*, 2009, **339**, 390–403.

82 P. Jarvis and J. Fawell, *Curr. Opin. Environ. Sci. Health*, 2021, **20**, 100239.

83 Q. Luo, S. Wang, L. Sun and H. Wang, *Sci. Rep.*, 2017, **7**, 39878.

84 A. M. Vindedahl, J. H. Strehlau, W. A. Arnold and R. L. Penn, *Environ. Sci.: Nano*, 2016, **3**, 494–505.

85 V. Poirier, C. Roumet and A. D. Munson, *Soil Biol. Biochem.*, 2018, **120**, 246–259.

86 A. Andreetta, M.-F. Dignac and S. Carnicelli, *Biogeochemistry*, 2013, **112**, 41–58.

87 F. Watteau, G. Villemin, G. Burtin and L. Jocteur-Monrozier, *Eur. J. Soil Sci.*, 2006, **57**, 247–257.

88 G. Bodner, D. Leitner and H.-P. Kaul, *Plant Soil*, 2014, **380**, 133–151.

89 D. A. Angers and J. Caron, *Biogeochemistry*, 1998, **42**, 55–72.

90 I. J. Gould, J. N. Quinton, A. Weigelt, G. B. De Deyn and R. D. Bardgett, *Ecol. Lett.*, 2016, **19**, 1140–1149.

91 N. Kandhol, M. Jain and D. K. Tripathi, *Physiol. Plant.*, 2022, **174**, e13665.

92 A. E. Ajayi and R. Horn, *Int. Agrophys.*, 2016, **30**, 391–399.

93 P. Hartmann, H. Fleige and R. Horn, *Geoderma*, 2009, **150**, 188–195.

94 A. E. Ajayi, D. Holthusen and R. Horn, *Soil Tillage Res.*, 2016, **155**, 166–175.

95 R. Lal, *Agron. J.*, 2020, **112**, 3265–3277.

96 D. Soltys-Kalina, J. Plich, D. Strzelczyk-Żyta, J. Śliwka and W. Marczewski, *Breed. Sci.*, 2016, **66**, 328–331.

97 N. Verbruggen and C. Hermans, *Amino Acids*, 2008, **35**, 753–759.

98 S. J. Klaine, P. J. J. Alvarez, G. E. Batley, T. F. Fernandes, R. D. Handy, D. Y. Lyon, S. Mahendra, M. J. McLaughlin and J. R. Lead, *Environ. Toxicol. Chem.*, 2008, **27**, 1825–1851.

99 T. M. Linh, N. C. Mai, P. T. Hoe, L. Q. Lien, N. K. Ban, L. T. T. Hien, N. H. Chau and N. T. Van, *J. Nanomater.*, 2020, **2020**, e4056563.

100 T. Ahmed, M. Noman, N. Manzoor, M. Shahid, M. Abdullah, L. Ali, G. Wang, A. Hashem, A.-B. F. Al-Arjani, A. A. Alqarawi, E. F. Abd Allah and B. Li, *Ecotoxicol. Environ. Saf.*, 2021, **209**, 111829.

101 Y.-T. Du, M.-J. Zhao, C.-T. Wang, Y. Gao, Y.-X. Wang, Y.-W. Liu, M. Chen, J. Chen, Y.-B. Zhou, Z.-S. Xu and Y.-Z. Ma, *BMC Plant Biol.*, 2018, **18**, 320.

